On the vibrational Born–Oppenheimer separation scheme for molecules with regular and chaotic states

Stavros C. FarantosJonathan Tennyson

Citation: **84**, (1986); doi: 10.1063/1.450764
View online: http://dx.doi.org/10.1063/1.450764
View Table of Contents: http://aip.scitation.org/toc/jcp/84/11
Published by the American Institute of Physics

On the vibrational Born–Oppenheimer separation scheme for molecules with regular and chaotic states

Stavros C. Farantos
Department of Chemisty, University of Crete and Institute of Electronic Structure and Laser, Research Centre of Crete, 711 10 Iraklion, Crete, Greece

Jonathan Tennyson
Department of Physics and Astronomy, University College London, Gower Street, London WC1E 6BT, United Kingdom

(Received 17 January 1986; accepted 11 February 1986)

Quantum mechanical calculations on KCN, LiCN, and ArHCl with two-dimensional (2D) potentials show that the Born–Oppenheimer separation scheme with the slow coordinate as the adiabatic variable is reliable for regular states but not for chaotic states. Three-dimensional (3D) calculations on KCN and ArHCl, where the coupling of CN or HCl motion with the other coordinates is introduced through the kinetic part of the Hamiltonian, demonstrate the existence of an extra constant of motion even for high excitations of the diatom. In 3D, cuts through the wave function show regular nodal patterns across the regular and chaotic coordinates. However, the number of nodes displaced by the chaotic coordinate varies for different values of the third constant coordinate. It is suggested that these plots provide a useful diagnostic aid for multidimensional irregular states. The adiabatic separation of regular motion gives results in excellent agreement with fully coupled 3D calculations.

I. INTRODUCTION

A striking feature of most molecules is the large number of regular, mode localized vibrational states supported by seemingly complicated potential functions. As the size of molecule that can be treated by fully mode coupled calculations is limited to triatomics and some tetraatomics, it is desirable to develop approximate methods which reflect this approximate mode separation. Such methods may also provide a useful starting point for understanding states for which an approximate mode separation is no longer valid. These mode coupled states are known to be closely associated with chaotic or irregular behavior.[1]

A method of mode decoupling which has been applied successfully to a number of problems is a Born–Oppenheimer (BO) separation of fast and slow vibrational modes.[2–7] Aquilanti *et al.*[3] and Taylor and co-workers[2] have demonstrated that the adiabatic potentials produced in the BO approximation can explain the astonishing regularity and localization of the wave functions found for the Henon–Heiles[8] and stadium[9] potentials even at very high energy.

Recently we have studied the classical and quantum dynamics of the floppy LiCN[10,11] and KCN[12] molecules using *ab initio* potential energy surfaces for the electronic ground state.[13,14] These calculations were performed by freezing the high frequency CN stretching coordinate. Similar calculations have also been presented for the van der Waals systems Ar–HCl.[15] Although these molecules were found to have a relatively low-lying onset of chaos, for LiCN a large number of regular states were found. Two such states are shown in Fig. 1; both these states lie above the barrier separating LiNC from metastable LiCN. This regularity is particularly striking since the potential does not presuppose any approximate separability of the stretching and bending motion.

For systems with two degrees of freedom, classical trajectories can either be classified as chaotic or regular according to whether M, the number of constants of motion, equals one or two. In N-dimensional systems with $N > 2$, the important intermediate case $1 < M < \mathrm{N}$ can arise. This was considered in a classical analysis of a generalized Henon–Heiles problem by Contopoulos *et al.*[16] For a fixed energy they were able to find regions of phase space with one, two, and three constants of motion. Despite the fact that the simplest vibrating molecule that can display chaos is the triatomic ($N = 3$), there is limited work which has explicitly considered this problem.

The inclusion of the extra degree of freedom, which was omitted in our previous calculations on KCN, in such a fashion that it remains regular in the energy region of interest, will allow us to consider directly the case intermediate between complete regularity and total chaos. For ArHCl, inclusion of the HCl stretch has been shown to be vital in obtaining reliable binding energies for the chaotic states of the van der Waals complex.[15]

In this paper we show that the regular solutions found in the 2D calculations of LiCN, KCN, and ArHCl are well described within the Born–Oppenheimer separation scheme. Three-dimensional calculations on KCN and ArHCl reveal classical and quantum methods of identifying the coordinate(s) that can be treated by using an adiabatic approximation.

II. THEORETICAL METHODS

The coordinates for a triatomic system A–BC are expressed as functions of the distance of A from the BC center of mass R, the BC bond length r, and ϑ the angle between **R** and **r**. The separable potential can then be written

$$V(r,R,\vartheta) = V(r) + V(R,\vartheta)\,, \tag{1}$$

 0021-9606/86/116210-08$02.10

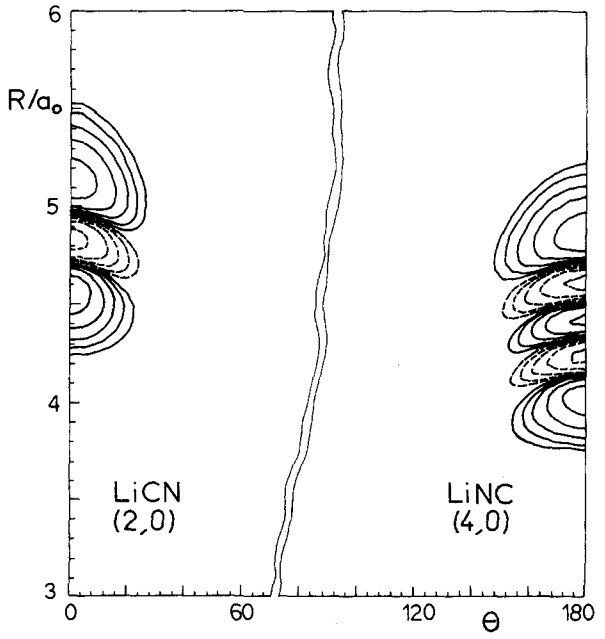

FIG. 1. Contour plots for two exact eigenfunctions (a) (4,0) of LiNC and (b) (2,0) of LiCN. (v_s,v_b) denotes the quantum numbers of the stretching and bending modes.

where $V(R,\vartheta)$ is the 2D potential used previously. For KCN and LiCN, $V(R,\vartheta)$ is an analytic Legendre polynomial representation of the *ab initio* data of Wormer *et al.*[13,14] These workers showed that for these molecules $V(R,\vartheta)$ was only weakly dependent on r. Similar assumptions have generally been made for van der Waals complexes. The ArHCl interaction potential is the empirical M5 potential of Hutson and Howard.[6(b)] In the 3D calculations, $V(r)$ is taken as a harmonic potential for CN, whereas HCl is described by the anharmonic empirical potential of Ogilvie.[17]

The Hamiltonian for the body-fixed rotationless problem can be written

$$H=\frac{p_r^2}{2\mu_d}+\frac{p_R^2}{2\mu}+\left(\frac{1}{2\mu_d r^2}+\frac{1}{2\mu R^2}\right)p_\vartheta^2+V(r,R,\vartheta)\,, \tag{2}$$

where

$$\mu_d^{-1}=m_B^{-1}+m_C^{-1}\,, \tag{3}$$

$$\mu^{-1}=m_A^{-1}+(m_B+m_C)^{-1}\,, \tag{4}$$

m_A, m_B, and m_C are the atomic masses. Coupling of the r coordinate with R and ϑ is through the kinetic part of the Hamiltonian.

The fully coupled 3D dynamical problem was solved classically by integrating Hamilton's equations in r, R, and ϑ and their conjugate momenta. The integration algorithm used was that of Shampine and Gordon.[18] As in our recent calculations on KCN,[12] initial conditions for R and ϑ coordinates and their conjugate momenta were selected by orthant sampling.[19] This involves the selection of unit random vectors in a four-dimensional space. Initial values for r and p_r were selected by specifying the harmonic action J, and angle, φ, variables:

$$r=\left(\frac{2J\hbar}{\mu_d\omega}\right)^{1/2}\cos\varphi\,, \tag{5}$$

$$p_r=-(2J\hbar\omega\mu_d)^{1/2}\sin\varphi\,, \tag{6}$$

where

$$J=v_{CN}+1/2\,.$$

ω is frequency and v_{CN} an integer quantum number.

Quantum mechanical 3D calculations were performed for KCN and ArHCl using program ATOMDIAT.[20]

An adiabatic separation of R and ϑ can be performed by taking ϑ as the adiabatic variable. For fixed values of ϑ we numerically solve the radial equation

$$\left[-\frac{\hbar^2}{2\mu}\frac{\partial^2}{\partial R^2}+V(R;\vartheta)\right]\Psi(R)=E_R^{v_s}(\vartheta)\Psi(R) \tag{7}$$

in order to estimate the stretching eigenvalues.[27] The eigenvalues of the angular part of Hamiltonian (2) are obtained by solving the equation

$$\left[-\frac{\hbar^2}{2}\left(\frac{1}{\mu_d r^2}+\frac{1}{\mu R^2}\right)\hat{l}^2+E_R^{v_s}(\vartheta)\right]\Phi(\vartheta)=E^{v_b}\Phi(\vartheta)\,, \tag{8}$$

where r and R are held fixed at their equilibrium values. $\hat{l}$ is the angular momentum operator which describes rotations of A around the center of mass of BC. Equation (8) is solved by expanding Φ in Legendre polynomials:

$$\Phi(\vartheta)=\sum_{j=0}^{n}a_j P_j(\cos\vartheta) \tag{9}$$

and diagonalizing the Hamiltonian matrix

$$H_{jj}=\left(\frac{1}{\mu_d r^2}+\frac{1}{\mu R^2}\right)j(j+1)\delta_{jj}+\langle P_j|E_R^{v_s}(\vartheta)|P_j\rangle\,. \tag{10}$$

If $E_R^{v_s}(\vartheta)$ is expanded in Legendre polynomials, the integral in Eq. (10) can be calculated analytically:

$$\langle P_{j'}|E_R^{v_s}|P_j\rangle=\sum_{\lambda=0}^{k}[(2j'+1)(2j+1)]^{1/2}\times E_{R\lambda}^{v_s}\begin{pmatrix}j' & \lambda & j\\ 0 & 0 & 0\end{pmatrix}^2, \tag{11}$$

where

$$\begin{pmatrix}j' & \lambda & j\\ 0 & 0 & 0\end{pmatrix}$$

are 3-j symbols.

III. RESULTS AND DISCUSSION

A. Adiabatic approximation in 2D systems

In a recent publication we calculated the first 80 levels of LiCN converged to 1 cm^{-1}.[10] Using several indicators to characterize the states as regular or irregular we have found that the stretching overtones with the bending mode in the ground state or excited with a few quanta show a striking regularity for both minima, LiNC (absolute) and LiCN (relative). Classical trajectories initialized with most of the energy in the stretching mode also show regularity, in agree-

TABLE I. Band origins (in cm^{-1}) for the rectangular approximation for LiNC and LiCN. The states are assigned v_s and v_b for excitation in the stretching and bending coordinates, respectively.

Rectangular		Variational[a]		
v_s	E	v_s,v_b	E	ΔE
		LiNC		
1	755.2	(1,0)	754.4	0.8
2	1499.9	(2,0)	1498.4	1.5
3	2234.1	(3,0)	2231.8	2.3
4	2957.6	(4,0)	2954.9	2.7
5	3670.4		...	...
		LiNC		
v_b				
1	307.9	(0,2)	247.2	60.7
2	635.1	(0,4)	469.0	166.1
3	973.4	(0,6)	665.6	307.8
4	1317.4	(0,8)	836.8	480.6
		LiCN		
v_s				
1	686.2	(1,0)	689.1	−2.9
2	1362.3	(2,0)	1368.5	−6.2
3	2028.2		...	...

[a] Reference 10.

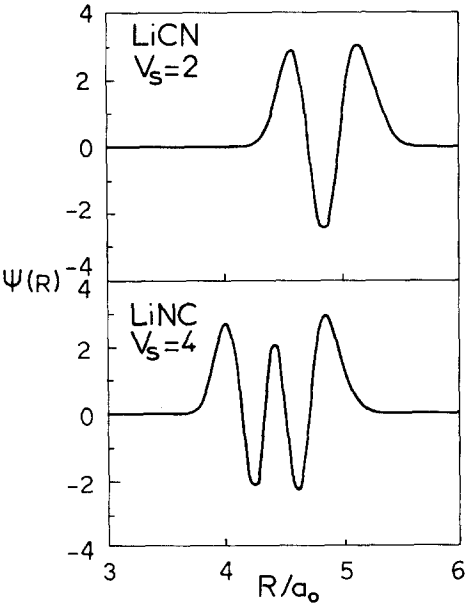

FIG. 2. The stretching wave functions in the rectangular approximation for (a) $v_s = 4$ of LiNC and (b) $v_s = 2$ of LiCN.

ment with the quantum results.[11] The high regularity and localization of the wave functions for the stretching overtones is clearly shown in the nodal patterns of the wave functions (Fig. 1). By numerically solving the radial equation (7) for $\vartheta = \pi$, and 0 we obtain the fundamental and stretching overtones of LiNC and LiCN. The results of this approximation which has been called rectangular,[2] are compared with the variationally exact results in Table I. Although the stretching eigenvalues are in good agreement, poor results are obtained for bending overtones. This could be anticipated since, as can be seen in Fig. 1 of Ref. 21, the potential strongly couples the stretching and bending coordinates for ϑ different than the equilibrium values 0 or π.

The accuracy of the rectangular approximation for the stretching overtones explains the localization of these states found in the variational wave functions. Figure 2 shows the stretching 1D wave functions of LiNC and LiCN for $v_s = 4$ and 2, respectively. The localization and position of the nodes are in agreement with those in Fig. 1.

A more sophisticated separation scheme is to apply a Born–Oppenheimer approximation to the vibrational coordinates. This can be done using either R or ϑ as the adiaba-

TABLE II. Comparison of LiNC ground state total energy and vibrational band origins (in cm^{-1}) for (A) variationally exact calculations (Ref. 10), and Born–Oppenheimer approximations with (B) ϑ and (C) R as the adiabatic variable.

v_b / v_s		0	2	4	6	8	10	12	14	16	18	20
A	0	−53 172.26	247.2	469.0	665.6	836.8	982.3	1111.7	1245.3	1390.3	1545.4	1708.4
B		−53 173.88	244.8	466.2	663.5	835.9	983.5	1118.5	1259.0	1409.4	1568.5	1734.9
C		−53 221.07	247.3	500.4								
A	1	754.4	998.1	1212.9	1397.7	1550.4	1671.5	1786.6				
B		749.4	980.8	1185.3	1362.0	1509.8	1635.7	1762.2				
C		570.1	828.8	1086.3								
A	2	1 498.4	1738.7	1946.4	2118.1	2246.8						
B		1 488.4	1706.0	1892.6	2046.0	2167.5						
C		940.8	1201.8	1458.4								
A	3	2 231.8	2469.0	2669.5	2825.4	2918.3						
B		2 216.7	2420.0	2586.9	2713.0	2810.5						
C		1 274.0	1547.5	1817.3								
A	4	2 954.9	3188.9	3424.3	3565.5							
B		2 934.3	3122.6	3266.3	3359.7							
C		1 639.0	1922.4	2196.7								

TABLE III. Born–Oppenheimer approximation with ϑ as the adiabatic coordinate for KCN. Excited state energies are given relative to the ground vibrational state.

	BO	Variational		
v_s	v_b	E (cm^{-1})	E (cm^{-1})	ΔE (cm^{-1})
0	0	− 38 866.66	− 38 861.40	− 5.26
0	1	119.9	116.1	− 3.8
0	2	226.0	217.8	− 8.2
1	0	288.7	294.3	5.6
0	3	318.4	314.6	− 3.8
0	4	395.8	379.6	16.2
1	1	411.3	420.5	− 9.2
0	5	458.2	448.4	9.8
1	2	520.5	494.9	25.6
0	6	522.2	530.4	− 8.2

TABLE IV. Born–Oppenheimer approximation with ϑ as the adiabatic coordinate for ArHCl.

	BO	Variational[a]		
v_s	v_b	E (cm^{-1})	E (cm^{-1})	ΔE (cm^{-1})
0	0	− 117.83	− 117.24	0.59
		(− 117.13)		
0	1	− 92.12	− 92.33	− 0.21
		(− 92.22)		
1	0	− 85.10	− 83.76	1.34
		(− 83.66)		
1	1	− 63.11	− 65.04	− 1.93
2	0	− 58.84	− 58.70	0.14
0	2	− 49.73	− 47.88	1.85
2	1	− 38.93	− 40.56	− 1.63
3	0	− 38.41	− 36.60	1.81
4	0	− 23.22	− 24.98	− 1.76
1	2	− 19.96	− 22.01	− 2.05
3	1	− 19.46	− 16.81	2.65
5	0	− 12.61	− 11.09	1.52
6	0	− 5.85	− 6.68	− 0.83
4	1	− 4.45	− 5.17	− 0.72

[a] Reference 15.

tic variable. Usually, but not always,[6(a)] the slow coordinate ϑ is taken as the adiabatic variable. A disadvantage of this method is that it is necessary to provide a value of R for kinetic term $(\mu R^2)^{-1}$, for which we used the equilibrium value. In our applications we found that other realistic values of R did not significantly alter our results. In the expansion of the adiabatic potentials $E_R^{v_s}(\vartheta)$ in Legendre polynomials we used $\lambda \leqslant 44$ which ensured an accurate representation of the potential.

Table II compares the results of the BO approximations with the essentially exact variational results of the coupled problem. The table also shows the values obtained using R as the adiabatic variable. It can be seen that the energy of these states are severely underestimated compared to the exact ones. This can be attributed to the fact that the adiabatic potential $E_\vartheta^{v_b}(R)$ is considerably broader than those obtained from Eq. (1) for $\vartheta = 0$ or π.

For the adiabatic ϑ BO approximation, Table II shows generally good agreement with the variational results. For the mode localized overtone $(v_s,0)$ and $(0,v_b)$ the errors in the band origins are less than 1%, similar to those found for calculations on model problems.[2,3] For the higher bending overtones and for the mode mixed combination levels the agreement is not as good. In particular, the order of the levels is not the same as that found in the full calculations, for example, compare the levels (0,16) and (1,6).

Because of the coupling in the potential between ϑ and R away from linear geometries, excitation of the bending mode increases the coupling with the stretching coordinate. For these mode coupled states the BO approximation is less reliable. In fact it is this coupling which leads to the irregular (chaotic) quantum states which have been found for LiCN.[10,11] Our results thus support the suggestion by Taylor and co-workers[1,2] that the regular (mode localized) states are the result of a separable zeroth order Hamiltonian.

Two-dimensional variational calculations on KCN show it to be a pathologically chaotic vibrator for which only the first three levels can be assigned good quantum numbers.[12] Table III compares adiabatic ϑ BO results with variationally exact levels. The comparison is upon an energy ordering basis. For the three low-lying regular states the BO results provide a good approximation to the exact answers. For the higher vibrational states these differences are generally larger and erratic.

Recent quantum mechanical calculations on the van der Waals system Ar–HCl[15] has shown erratic behavior for states which are bound by less than 40 cm^{-1} and that this erratic behavior is strongly coupled to the HCl stretching motion. In the next section we show that classical dynamics predicts an early onset of chaos similarly to KCN molecule.

In Table IV we compare the BO results for ArHCl with variational ones. The values in parenthesis are those obtained by Hutson and Howard.[6(b)]. The small differences between these and our values should be attributed to the omission of the adiabatic correction term

$$\left\langle \Psi_i \left| \frac{\partial^2}{\partial \theta^2} \right| \Psi_i \right\rangle$$

in our calculations. Apart from the fact that the agreement deteriorates as the energy increases, we can see that in the BO approximation some resonances are predicted for the states above − 40 cm^{-1}. These are the (2 1), (3 0) and (1 2), (3 1) pair of states and are indicated by braces.

B. Adiabaticity in systems with three degrees of freedom

Describing the CN oscillations with a harmonic potential [Eq. (1)] we have studied trajectories in the six-dimensional phase space of KCN. $V(r)$ is the same as that used for rovibrational calculations on KCN by Tennyson and Sutcliffe.[22] The equilibrium bond length is $r = 2.186a_0$ and force constant $k = 0.172$ μN Å. This gives a fundamental frequency of 2129.7 cm^{-1} for the CN stretch.

We have studied trajectories for several CN levels of excitation. The energy in the R, ϑ coordinates was taken in the same range as in Ref. 12. For all trajectories studied, we found sharp caustics, in the projection onto the (r,R) and

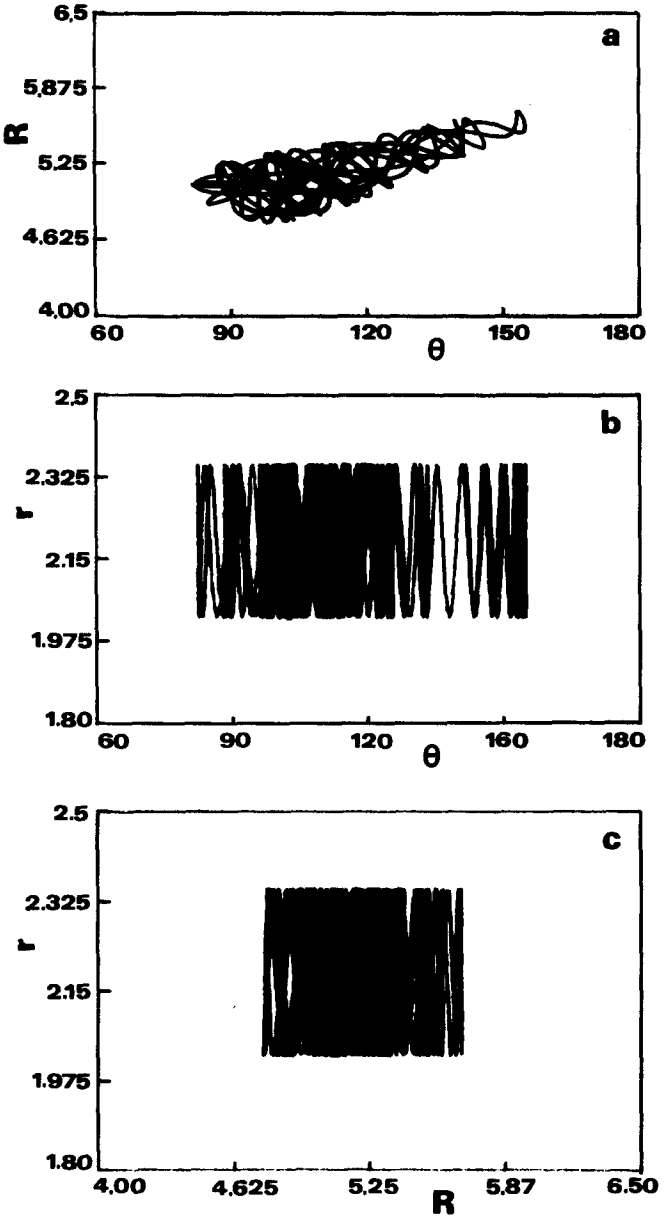

FIG. 3. Projections of a trajectory of KCN on the three different coordinate planes with $v_{CN} = 1$ and the energy in the other coordinates is 464 cm^{-1}.

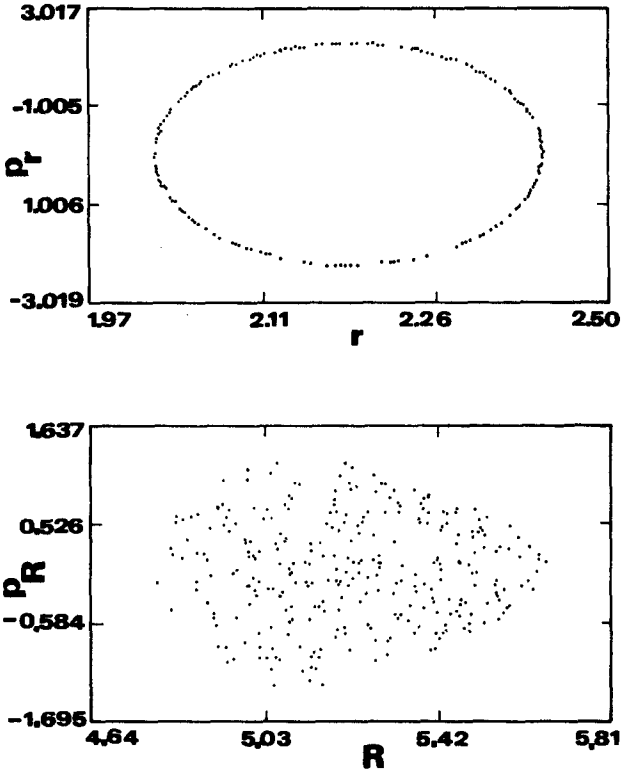

FIG. 4. Generalized Poincaré surfaces of section for the the same trajectory of Fig. 3.

(r,ϑ) coordinate planes and chaotic patterns in the (R,ϑ) plane. Figure 3 shows a trajectory with $v_{CN} = 1$ and excitation energy for the other coordinates equal to 464 cm^{-1}. In spite of the sharp caustics in Figs. 3(b) and 3(c) the trajectory does not uniformly cover the available space. This behavior persists even when the CN bond is excited above the dissociation limit of KCN.

A better method of displaying trajectories in a multidimensional configuration space is to use Wolf and Hase's[23] generalization of the Poincaré surface of section. For each coordinate they plotted (x, p_x) every time the trajectory passed through a particular plane in a certain direction. The near harmonic motion of CN is shown by plotting (r, p_r) for the plane $R = R_e$ (Fig. 4). On the other hand, plots of (R, p_R) and (ϑ, p_ϑ) definitely show the chaotic nature of these coordinates. All these trajectories have two constants of motion and chaos appears because of the R,ϑ coupling. This is best demonstrated by calculating the maximal Lyapunov characteristic number (MLCN). As shown in Table V, we reproduce the average MLCN found in 2D calculations with r frozen (Ref. 12).

The quantum mechanical calculation for 3D KCN were performed by augmenting the 2D basis used by Tennyson and Sutcliffe for the low-lying levels of KCN[24] with four Morse oscillator-like functions with $r_e = 2.465a_0$, $D_e = 0.1045E_h$, and $\omega_e = 0.0120E_h$ which gave a good representation of the r coordinate.[25]

The KCN vibrational wave functions were analyzed by taking contour plots of the amplitude for two coordinates q_1,

TABLE V. Average maximal Lyapunov characteristic numbers after integrating ten pairs of trajectories for KCN. Values in parentheses are the results of two-dimensional calculations with the same $E_{R,\vartheta}$ (Ref. 12).

v_{CN}	E_{CN} (cm^{-1})	$E_{R,\vartheta}$ (cm^{-1})	MLCN (ps^{-1})
0	1 065	205	0.8 ± 0.3
			(0.6 ± 0.3)
0	1 065	394	2.6 ± 0.3
			(2.6 ± 0.3)
0	1 065	542	4.2 ± 0.1
2	5 323	542	4.1 ± 0.4
5	11 711	542	4.5 ± 0.5
18	39 400	542	5.0 ± 0.5
			(4.2 ± 0.4)

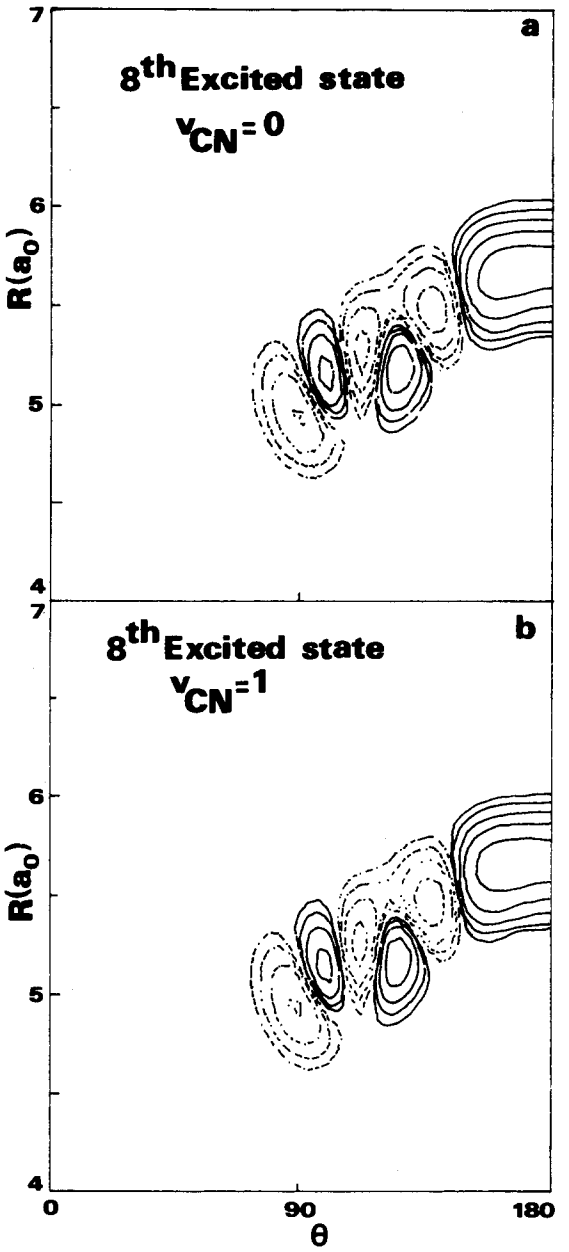

FIG. 5. Nodal structure of two states of KCN (a) $v_{CN} = 0$ and (b) $v_{CN} = 1$.

q_2 and a fixed value for the third coordinate, q_3. We designate such a plot $(q_1,q_2)_{q_3}$. Plots $(R,\vartheta)_{r_0}$, with r frozen at its equilibrium point $r_0 = 2.186a_0$, showed that the low-lying states, well below the threshold to CN excitation, were indistinguishable from those obtained by solving the 2D problem with r fixed at r_0, see Ref. 12. For all these levels plots of (ϑ,r) and (R,r) showed no nodes in the r coordinate.

Above the threshold to CN excitation the plots $(\vartheta,r)_R$ and $(R,r)_\vartheta$ either show one or no nodes in the r coordinate. The $(R,\vartheta)_{r_0}$ plots showed the states with no nodes to be highly excited in R and ϑ (and probably poorly represented at large R). Plots of $(R,\vartheta)_{r_0}$ for the states with one r node were indistinguishable from the $(R,\vartheta)_{r_0}$ plots for the lowest vibrational levels, see Fig. 5.

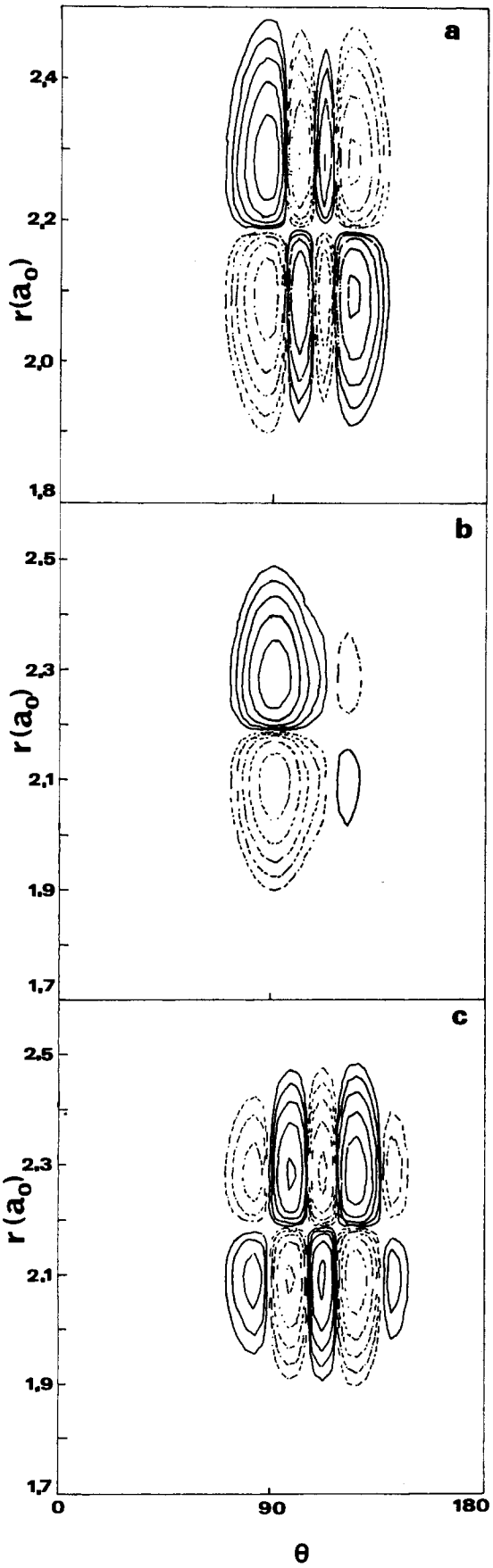

FIG. 6. Nodal structure of the eighth state of KCN for three different constant values of R. (a) $R = 5.0$, (b) $R = 4.8$, and (c) $R = 5.2a_0$.

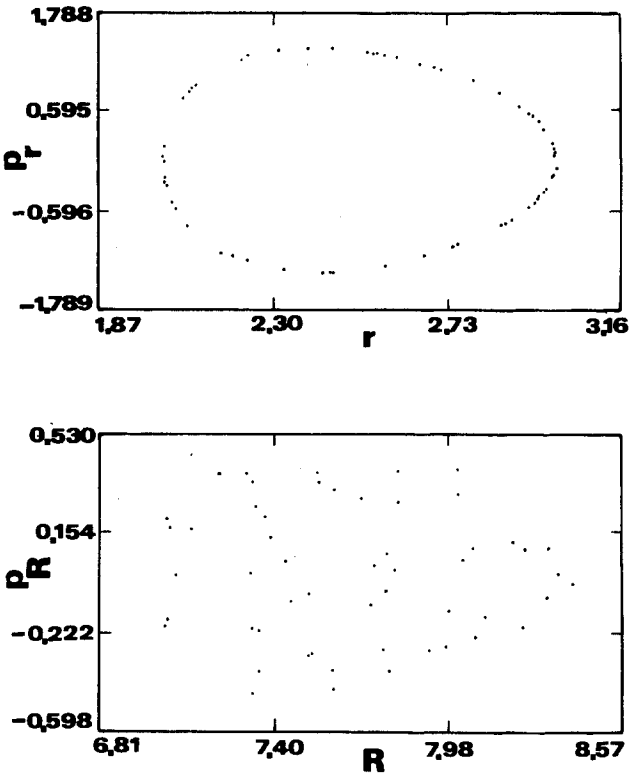

FIG. 7. Generalized Poincaré surfaces of section for a trajectory of ArHCl. $v_{HCl} = 2$ and energy in (R,ϑ) modes equals 63 cm^{-1}.

Analysis of the nodal structure of the $(R,\vartheta)_r$ plots show most of the states to have the complicated nodal structure which has been associated with chaos.[10–12,15] Conversely all the plots of $(r,R)_\vartheta$ and $(r,\vartheta)_R$ have clear nodal lines and thus superficially, allow quantum numbers to be assigned.

TABLE VI. Comparison of fully coupled 3D calculations (Ref. 15) with 2D Born–Oppenheimer results for the vibrational levels of ArHCl. Energies (in cm^{-1}) are relative to free Ar and HCl (v_{HCl}).

$v_{HCl} = 0$[a]		$v_{HCl} = 1$[b]	
3D[c]	BO	3D	BO
− 117.15	− 117.15	− 117.49	− 117.49
− 92.23	− 92.23	− 92.61	− 92.61
− 83.68	− 83.68	− 83.98	− 83.98
− 64.91	− 64.91	− 65.42	− 65.42
− 58.61	− 58.61	− 58.97	− 58.98
− 47.56	− 47.54	− 48.85	− 48.85
− 40.43	− 40.43	− 40.95	− 40.95
− 36.50	− 36.49	− 36.89	− 36.89
− 24.78	− 24.76	− 25.64	− 25.64
− 21.94	− 21.94	− 22.19	− 22.20
− 16.58	− 16.57	− 17.49	− 17.49
− 11.02	− 11.00	− 11.30	− 11.30
− 6.51	− 6.51	− 7.22	− 7.22
− 5.11	− 5.03	− 5.27	− 5.28
		− 0.69	− 0.69

[a] For $v_{HCl} = 0$, $E_0 = -35\,750.37$, and $\langle r \rangle = 2.4260 a_0$.
[b] For $v_{HCl} = 1$, $E_0 = -32\,863.69$, and $\langle r \rangle = 2.4619 a_0$.
[c] These results supersede those given in Ref. 15.

Varying the fixed coordinate, however, reveals the true nature of these states. Comparison of plots of $(r,\vartheta)_R$ with $R = 4.8$, 5.0, and $5.2 a_0$ show that, for states the $(R,\vartheta)_r$ plots indicate to be chaotic, the quantum numbers assigned to the ϑ coordinate differ for each R, see Fig. 6. Similarly plots $(r,R)_\vartheta$ with $\vartheta = \vartheta_1$ and ϑ_2 show changes in the R coordinate quantum numbers. In contrast, the r quantum numbers are independent of which cut through the wave function is taken.

Classical calculations have been carried out for a 3D ArHCl potential. As in KCN, an early onset to chaotic behavior (below the quantum zero point energy) is observed, related to the coupling of the R,ϑ coordinates. On the other hand, regularity remains in the r coordinate even for high excitation of HCl (Fig. 7). Plots of 3D quantum mechanical calculations on ArHCl show regularity in r coordinate in the same fashion as KCN.

This behavior suggests that an adiabatic representation of the HCl coordinate should be able to reproduce the complicated behavior observed previously in the fully coupled 3D calculations. We have thus performed adiabatic calculations on ArHCl. Because of the assumed separability of the potential, these simply involve using the correctly averaged value of r:

$$\langle r \rangle = [\langle v|r^{-2}|v\rangle]^{-1/2} \tag{12}$$

in the angular kinetic energy term of Eq. (2), for HCl in the v vibrational state. Table VI shows that this approximation reproduces all the binding energies of the full calculation to with 0.02 cm^{-1}, despite shifts several hundredfold larger for different HCl vibrational states. The adiabatic separation is thus seen to be very powerful.

IV. CONCLUSIONS

The adiabatic Born–Oppenheimer approximation as a separation scheme for coupled multidimensional systems has been tested in the light of classification of states as regular or chaotic. Comparison of Born–Oppenheimer results with previous fully coupled variational 2D calculations on LiCN, KCN, and ArHCl demonstrates that for regular states a satisfactory agreement is obtained but the reliability of the adiabatic separation scheme is lost when irregular (strongly coupled) states are encountered.

Three-dimensional classical and quantum calculations on KCN and ArHCl show that when the coupling of CN or HCl motion with the other coordinates is introduced via the kinetic terms in the Hamiltonian, the action variable related to these diatomics is conserved. Inspection of the trajectories or wave functions reveal the coordinate related to an extra constant of motion or the existence of a good quantum number. However the complications in nodal patterns which arises in the case of resonances[26] weakens this pictorial method.

Particularly, a chaotic component manifests itself in the same way as in the independent 2D calculations. This is quantitatively manifested by the maximal Lyapunov characteristic numbers. In systems with three degrees of freedom, where there are two good quantum numbers, the misleading regularity of the nodal patterns which appears in cuts

through the wave function for one regular and one chaotic coordinate is revealed by the change in the number of nodes in the chaotic coordinate for different constant values of the third coordinate. In the above situation the adiabatic separation of the regular coordinate gives results in good agreement with exact variational results even for cases where a rectangular approximation is poor. For ArHCl, an adiabatic representation of the HCl coordinate is shown to give a very accurate representation of the often erratic shifts in van der Waals binding energy with HCl vibrational state.

Dynamical calculations, mainly classical, in triatomic systems have shown that regular trajectories persist at high energies of excitation; even above a dissociation barrier.[23] For these regular states as well as for molecules of high dimensionality we anticipate that Born–Oppenheimer separation methods will be increasingly useful.

[1]G. Hose and H. S. Taylor, Chem. Phys. **84**, 375 (1984).
[2]G. Hose, H. S. Taylor, and A. Tip, J. Phys. A **17**, 1203 (1984); H. S. Taylor, in *Multiphoton Processes*, edited by P. Lambropoulos and S. J Smith (Springer, Berlin, 1984); K. Stefanski and H. S. Taylor, Phys. Rev. A **31**, 2821 (1985).
[3]V. Aquilanti, S. Cavalli, and G. Crossi, in *Chaotic Behavior in Quantum Systems. Theory and Application*, edited by G. Casati (Plenum, New York, 1985), p. 299.
[4]H. Ramanowski and J. M. Bowman, Chem. Phys. Lett. **110**, 235 (1984).
[5]S. L. Holmgren, M. Waldman, and W. Klemperer, J. Chem. Phys. **67**, 4414 (1977).
[6](a) J. M. Hutson and B. J. Howard, Mol. Phys. **41**, 1123 (1981); (b) **45**, 769 (1982).
[7]J. Makarewicz, J. Mol. Spectrosc. **105**, 1 (1984); J. Makarewicz and A. Wierzbicki, Chem. Phys. Lett. **108**, 155 (1984).
[8]M. Henon and C. Heiles, Astron. J. **69**, 73 (1973).
[9]S. W. McDonald and A. N. Kaufman, Phys. Rev. Lett. **42**, 1189 (1979); M. V. Berry, J. Phys. A **10**, 2083 (1977).
[10]S. C. Farantos and J. Tennyson, J. Chem. Phys. **82**, 800 (1985).
[11]J. Tennyson and S. C. Farantos, Chem. Phys. **93**, 237 (1985).
[12]J. Tennyson and S. C. Farantos, Chem. Phys. Lett. **109**, 160 (1984).
[13]R. Essers, J. Tennyson, and P. E. S. Wormer, Chem. Phys. Lett. **89**, 223 (1982).
[14]P. E. S. Wormer and J. Tennyson, J. Chem. Phys. **75**, 1245 (1981).
[15]J. Tennyson, Mol. Phys. **55**, 463 (1985).
[16]G. Contopoulos, L. Galgani, and A. Giorgilli, Phys. Rev. A **18**, 1183 (1978).
[17]J. F. Ogilvie, Proc. R. Soc. London Ser. A **378**, 287 (1981).
[18]L. F. Shampine and M. K. Gordon, *Computer Solutions of Ordinary Differential Equations* (Freeman, San Francisco, 1975).
[19]D. L. Bunker and W. L. Hase, J. Chem. Phys. **59**, 4621 (1973).
[20]J. Tennyson, Comput. Phys. Commun. **29**, 263 (1983); **32**, 109 (1984).
[21]G. Brocks and J. Tennyson, J. Mol. Spectrosc. **99**, 263 (1983).
[22]J. Tennyson and B. T. Sutcliffe, Mol. Phys. **46**, 97 (1982).
[23]R. J. Wolf and W. L. Hase, J. Chem. Phys. **73**, 3775 (1980).
[24]J. Tennyson and B. T. Sutcliffe, J. Chem. Phys. **77**, 4061 (1982).
[25]J. Tennyson, Comput. Phys. Rep. (in press).
[26]N. DeLeon, M. J. Davis, and E. J. Heller, J. Chem. Phys. **80**, 794 (1984).
[27]v_s and v_b denote the stretching and bending quantum numbers, respectively.